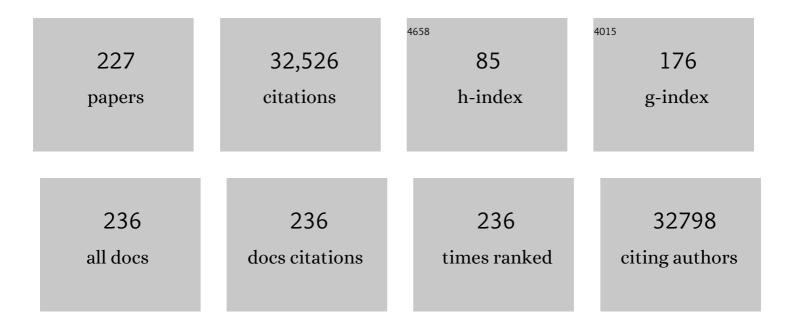
## Jin-Song Hu

List of Publications by Year in descending order

Source: https://exaly.com/author-pdf/5395572/publications.pdf Version: 2024-02-01



#	Article	IF	CITATIONS
1	Investigation of weak interlayer coupling in 2D layered GeS2 from theory to experiment. Nano Research, 2022, 15, 1013-1019.	10.4	11
2	Rational confinement engineering of <scp>MOF</scp> â€derived carbonâ€based electrocatalysts toward <scp>CO<sub>2</sub></scp> reduction and <scp>O<sub>2</sub></scp> reduction reactions. InformaÄnÃ-Materiály, 2022, 4, .	17.3	58
3	Synergistic Electrocatalysts for Alkaline Hydrogen Oxidation and Evolution Reactions. Advanced Functional Materials, 2022, 32, 2107479.	14.9	66
4	Hole transporting materials in inorganic CsPbI3â^'Br solar cells: Fundamentals, criteria and opportunities. Materials Today, 2022, 52, 250-268.	14.2	20
5	Strain relaxation and domain enlargement <i>via</i> phase transition towards efficient CsPbl <sub>2</sub> Br solar cells. Journal of Materials Chemistry A, 2022, 10, 3513-3521.	10.3	11
6	Copper-nickel rubeanate metal-organic framework, a new highly stable and long active life nanocomposite for high-performance supercapacitors. Journal of Materiomics, 2022, 8, 843-851.	5.7	2
7	Boronâ€∓ethering and Regulative Electronic States Around Iridium Species for Hydrogen Evolution. Advanced Functional Materials, 2022, 32, .	14.9	35
8	Electrocatalytic Hydrogen Oxidation in Alkaline Media: From Mechanistic Insights to Catalyst Design. ACS Nano, 2022, 16, 5153-5183.	14.6	46
9	Solution-processed Ge( <scp>ii</scp> )-based chalcogenide thin films with tunable bandgaps for photovoltaics. Chemical Science, 2022, 13, 5944-5950.	7.4	4
10	Nickel/cobalt/copper sulfide dodecahedral hollow multi-shelled structures, characterization, and application as a suitable nanomaterial for high-performance supercapacitors. Electrochimica Acta, 2022, 420, 140437.	5.2	5
11	Coordination anchoring synthesis of high-density single-metal-atom sites for electrocatalysis. Coordination Chemistry Reviews, 2022, 466, 214603.	18.8	21
12	Rational design of integrated electrodes for advancing high-rate alkaline electrolytic hydrogen production. Journal of Materials Chemistry A, 2022, 10, 12764-12787.	10.3	10
13	Regulating surface In–O in In@InO core-shell nanoparticles for boosting electrocatalytic CO2 reduction to formate. Chinese Journal of Catalysis, 2022, 43, 1674-1679.	14.0	17
14	Crystallization Kinetics Modulation of FASnI <sub>3</sub> Films with Preâ€nucleation Clusters for Efficient Leadâ€Free Perovskite Solar Cells. Angewandte Chemie - International Edition, 2021, 60, 3693-3698.	13.8	80
15	A sulfur-rich small molecule as a bifunctional interfacial layer for stable perovskite solar cells with efficiencies exceeding 22%. Nano Energy, 2021, 79, 105462.	16.0	72
16	Crystallization Kinetics Modulation of FASnI <sub>3</sub> Films with Preâ€nucleation Clusters for Efficient Leadâ€Free Perovskite Solar Cells. Angewandte Chemie, 2021, 133, 3737-3742.	2.0	20
17	In-plane anisotropic 2D Ge-based binary materials for optoelectronic applications. Chemical Communications, 2021, 57, 565-575.	4.1	19
18	An antibonding valence band maximum enables defect-tolerant and stable GeSe photovoltaics. Nature Communications, 2021, 12, 670.	12.8	58

#	Article	IF	CITATIONS
19	Multiâ€Phase Heterostructure of CoNiP/Co <i><sub>x</sub></i> P for Enhanced Hydrogen Evolution Under Alkaline and Seawater Conditions by Promoting H <sub>2</sub> O Dissociation. Small, 2021, 17, e2007557.	10.0	83
20	Strain in perovskite solar cells: origins, impacts and regulation. National Science Review, 2021, 8, nwab047.	9.5	127
21	Recent Advances on Nonprecious-Metal-Based Bifunctional Oxygen Electrocatalysts for Zinc–Air Batteries. Energy & Fuels, 2021, 35, 6380-6401.	5.1	48
22	Regulating Fe-spin state by atomically dispersed Mn-N in Fe-N-C catalysts with high oxygen reduction activity. Nature Communications, 2021, 12, 1734.	12.8	488
23	Boosting the efficiency of GeSe solar cells by low-temperature treatment of p-n junction. Science China Materials, 2021, 64, 2118-2126.	6.3	24
24	Electrical Loss Management by Molecularly Manipulating Dopantâ€free Poly(3â€hexylthiophene) towards 16.93 % CsPbI <sub>2</sub> Br Solar Cells. Angewandte Chemie, 2021, 133, 16524-16529.	2.0	18
25	Electrical Loss Management by Molecularly Manipulating Dopantâ€free Poly(3â€hexylthiophene) towards 16.93 % CsPbl <sub>2</sub> Br Solar Cells. Angewandte Chemie - International Edition, 2021, 60, 16388-16393.	13.8	57
26	Molecular Linking Stabilizes Bi Nanoparticles for Efficient Electrochemical Carbon Dioxide Reduction. Journal of Physical Chemistry C, 2021, 125, 12699-12706.	3.1	6
27	Interfacial Strain Engineering in Wide-Bandgap GeS Thin Films for Photovoltaics. Journal of the American Chemical Society, 2021, 143, 9664-9671.	13.7	36
28	Carrier management makes perovskite solar cells approaching Shockley-Queisser limit. Science Bulletin, 2021, 66, 1372-1374.	9.0	12
29	Well-defined heteronuclear bimetallic atomic clusters: Emerging electrocatalysts. Fundamental Research, 2021, 1, 461-465.	3.3	10
30	Selective Se doping of NiFe2O4 on an active NiOOH scaffold for efficient and robust water oxidation. Chinese Journal of Catalysis, 2021, 42, 1395-1403.	14.0	51
31	Engineering carbon-shells of M@NC bifunctional oxygen electrocatalyst towards stable aqueous rechargeable Zn-air batteries. Chemical Engineering Journal, 2021, 418, 129409.	12.7	35
32	Confinement Strategies for Precise Synthesis of Efficient Electrocatalysts from the Macroscopic to the Atomic Level. Accounts of Materials Research, 2021, 2, 907-919.	11.7	46
33	Dual-Sites Tandem Catalysts for C–N Bond Formation via Electrocatalytic Coupling of CO <sub>2</sub> and Nitrogenous Small Molecules. , 2021, 3, 1468-1476.		50
34	Boosting Nitrogen Reduction to Ammonia on FeN <sub>4</sub> Sites by Atomic Spin Regulation. Advanced Science, 2021, 8, e2102915.	11.2	64
35	Surface reconstruction on silver nanoparticles decorated trimetallic hydroxide nanosheets to generate highly active oxygen-deficient (oxy)hydroxide layer for high-efficient water oxidation. Chemical Engineering Journal, 2021, 425, 131662.	12.7	19
36	MWCNT-mesoporous silica nanocomposites inserted in a polyhedral metal–organic framework as an advanced hybrid material for energy storage device. New Journal of Chemistry, 2021, 45, 18090-18101.	2.8	4

#	Article	IF	CITATIONS
37	Engineering inorganic lead halide perovskite deposition toward solar cells with efficiency approaching 20%. Aggregate, 2021, 2, 66-83.	9.9	24
38	Regulating the crystalline phase of intermediate films enables FA <sub>1â^'<i>x</i></sub> MA <sub><i>x</i></sub> PbI <sub>3</sub> perovskite solar cells with efficiency over 22%. Journal of Materials Chemistry A, 2021, 9, 24064-24070.	10.3	20
39	Investigation of the sublimation mechanism of GeSe and GeS. Chemical Communications, 2021, 57, 11461-11464.	4.1	5
40	Molecular Engineering for Bottom-Up Construction of High-Performance Non-Precious-Metal Electrocatalysts with Well-Defined Active Sites. Journal of Physical Chemistry C, 2021, 125, 22397-22420.	3.1	17
41	Steering elementary steps towards efficient alkaline hydrogen evolution via size-dependent Ni/NiO nanoscale heterosurfaces. National Science Review, 2020, 7, 27-36.	9.5	192
42	Strain-engineering the in-plane electrical anisotropy of GeSe monolayers. Physical Chemistry Chemical Physics, 2020, 22, 914-918.	2.8	16
43	GeSe thin-film solar cells. Materials Chemistry Frontiers, 2020, 4, 775-787.	5.9	75
44	Advanced transition metal/nitrogen/carbon-based electrocatalysts for fuel cell applications. Science China Chemistry, 2020, 63, 1517-1542.	8.2	56
45	Molecularly Engineered Strong Metal Oxide–Support Interaction Enables Highly Efficient and Stable CO <sub>2</sub> Electroreduction. ACS Catalysis, 2020, 10, 13227-13235.	11.2	94
46	Sustainable synthesis of supported metal nanocatalysts for electrochemical hydrogen evolution. Chinese Journal of Catalysis, 2020, 41, 1791-1811.	14.0	80
47	Regulating the charge diffusion of two-dimensional cobalt–iron hydroxide/graphene composites for high-rate water oxidation. Journal of Materials Chemistry A, 2020, 8, 11573-11581.	10.3	18
48	Synergistic Modulation of Non-Precious-Metal Electrocatalysts for Advanced Water Splitting. Accounts of Chemical Research, 2020, 53, 1111-1123.	15.6	315
49	Metastable Rock Salt Oxide-Mediated Synthesis of High-Density Dual-Protected M@NC for Long-Life Rechargeable Zinc–Air Batteries with Record Power Density. Journal of the American Chemical Society, 2020, 142, 7116-7127.	13.7	147
50	Mesoporous carbon confined intermetallic nanoparticles as highly durable electrocatalysts for the oxygen reduction reaction. Journal of Materials Chemistry A, 2020, 8, 15822-15828.	10.3	58
51	Regulating strain in perovskite thin films through charge-transport layers. Nature Communications, 2020, 11, 1514.	12.8	346
52	Microscopic investigations on the surface-state dependent moisture stability of a hybrid perovskite. Nanoscale, 2020, 12, 7759-7765.	5.6	12
53	Rationally Designed Three-Dimensional N-Doped Graphene Architecture Mounted with Ru Nanoclusters as a High-Performance Air Cathode for Lithium–Oxygen Batteries. ACS Sustainable Chemistry and Engineering, 2020, 8, 6109-6117.	6.7	28
54	Molecular Evidence for Metallic Cobalt Boosting CO <sub>2</sub> Electroreduction on Pyridinic Nitrogen. Angewandte Chemie, 2020, 132, 4944-4949.	2.0	29

#	Article	IF	CITATIONS
55	Roomâ€Temperature Solutionâ€Processed PbS Quantum Dot Solar Cells. Chinese Journal of Chemistry, 2020, 38, 356-360.	4.9	6
56	Phosphorus-doping activates carbon nanotubes for efficient electroreduction of nitrogen to ammonia. Nano Research, 2020, 13, 1376-1382.	10.4	61
57	Molecular Evidence for Metallic Cobalt Boosting CO <sub>2</sub> Electroreduction on Pyridinic Nitrogen. Angewandte Chemie - International Edition, 2020, 59, 4914-4919.	13.8	126
58	Organic Small Molecule Activates Transition Metal Foam for Efficient Oxygen Evolution Reaction. Advanced Materials, 2020, 32, e1906015.	21.0	56
59	Fe-doped Co <sub>3</sub> O <sub>4</sub> polycrystalline nanosheets as a binder-free bifunctional cathode for robust and efficient zinc–air batteries. Chemical Communications, 2020, 56, 5374-5377.	4.1	36
60	Engineering Mo/Mo <sub>2</sub> C/MoC hetero-interfaces for enhanced electrocatalytic nitrogen reduction. Journal of Materials Chemistry A, 2020, 8, 8920-8926.	10.3	54
61	Self atalyzed Growth of Co–N–C Nanobrushes for Efficient Rechargeable Zn–Air Batteries. Small, 2020, 16, e2001171.	10.0	84
62	Highâ€Efficiency CsPbI <sub>2</sub> Br Perovskite Solar Cells with Dopantâ€Free Poly(3â€hexylthiophene) Hole Transporting Layers. Advanced Energy Materials, 2020, 10, 2000501.	19.5	69
63	Progress in the Mechanisms and Materials for CO <sub>2</sub> Electroreduction toward C <sub>2+</sub> Products. Wuli Huaxue Xuebao/ Acta Physico - Chimica Sinica, 2020, 36, 1906085-0.	4.9	38
64	Recent Progress in Proton-Exchange Membrane Fuel Cells Based on Metal-Nitrogen-Carbon Catalysts. Wuli Huaxue Xuebao/ Acta Physico - Chimica Sinica, 2020, .	4.9	21
65	Autogenous Growth of Hierarchical NiFe(OH) <i><sub>x</sub></i> /FeS Nanosheetâ€Onâ€Microsheet Arrays for Synergistically Enhanced Highâ€Output Water Oxidation. Advanced Functional Materials, 2019, 29, 1902180.	14.9	179
66	Pore-structure-directed CO <sub>2</sub> electroreduction to formate on SnO <sub>2</sub> /C catalysts. Journal of Materials Chemistry A, 2019, 7, 18428-18433.	10.3	59
67	Identification of FeN <sub>4</sub> as an Efficient Active Site for Electrochemical N <sub>2</sub> Reduction. ACS Catalysis, 2019, 9, 7311-7317.	11.2	220
68	Investigation of Oxygen Passivation for High-Performance All-Inorganic Perovskite Solar Cells. Journal of the American Chemical Society, 2019, 141, 18075-18082.	13.7	120
69	Roomâ€Temperature Sustainable Synthesis of Selected Platinum Group Metal (PGM = Ir, Rh, and Ru) Nanocatalysts Wellâ€Dispersed on Porous Carbon for Efficient Hydrogen Evolution and Oxidation. Small, 2019, 15, e1903057.	10.0	93
70	Hetero-coupling of a carbonate hydroxide and sulfide for efficient and robust water oxidation. Journal of Materials Chemistry A, 2019, 7, 21959-21965.	10.3	28
71	Fe/P dual doping boosts the activity and durability of CoS <sub>2</sub> polycrystalline nanowires for hydrogen evolution. Journal of Materials Chemistry A, 2019, 7, 5195-5200.	10.3	78
72	Three-Dimensional Optical Anisotropy of Low-Symmetry Layered GeS. ACS Applied Materials & Interfaces, 2019, 11, 24247-24253.	8.0	27

Jin-Song Hu

#	Article	lF	CITATIONS
73	Temperature-Dependent Local Electrical Properties of Organic–Inorganic Halide Perovskites: In Situ KPFM and c-AFM Investigation. ACS Applied Materials & Interfaces, 2019, 11, 21627-21633.	8.0	42
74	A Rutile TiO 2 Electron Transport Layer for the Enhancement of Charge Collection for Efficient Perovskite Solar Cells. Angewandte Chemie, 2019, 131, 9514-9518.	2.0	10
75	A Rutile TiO <sub>2</sub> Electron Transport Layer for the Enhancement of Charge Collection for Efficient Perovskite Solar Cells. Angewandte Chemie - International Edition, 2019, 58, 9414-9418.	13.8	124
76	Cascade anchoring strategy for general mass production of high-loading single-atomic metal-nitrogen catalysts. Nature Communications, 2019, 10, 1278.	12.8	591
77	NiS <sub>2</sub> nanodotted carnation-like CoS <sub>2</sub> for enhanced electrocatalytic water splitting. Chemical Communications, 2019, 55, 3781-3784.	4.1	56
78	Chemical state of surrounding iron species affects the activity of Fe-Nx for electrocatalytic oxygen reduction. Applied Catalysis B: Environmental, 2019, 251, 240-246.	20.2	101
79	Single-Crystalline Nanosheets of Hybrid Perovskite Fabricated by a Vapor-Solution Sequential Deposition Route. Journal of Nanoscience and Nanotechnology, 2019, 19, 3669-3672.	0.9	0
80	Se-Doping Activates FeOOH for Cost-Effective and Efficient Electrochemical Water Oxidation. Journal of the American Chemical Society, 2019, 141, 7005-7013.	13.7	460
81	Synergy Effect of Both 2,2,2â€Trifluoroethylamine Hydrochloride and SnF <sub>2</sub> for Highly Stable FASnI <sub>3â^'x</sub> Cl <sub>x</sub> Perovskite Solar Cells. Solar Rrl, 2019, 3, 1800290.	5.8	45
82	Polarizationâ€ <del>S</del> ensitive Ultraviolet Photodetection of Anisotropic 2D GeS <sub>2</sub> . Advanced Functional Materials, 2019, 29, 1900411.	14.9	120
83	Negligibleâ€Pbâ€Waste and Upscalable Perovskite Deposition Technology for Highâ€Operationalâ€Stability Perovskite Solar Modules. Advanced Energy Materials, 2019, 9, 1803047.	19.5	68
84	Weak Interlayer Interaction in 2D Anisotropic GeSe <sub>2</sub> . Advanced Science, 2019, 6, 1801810.	11.2	40
85	Band engineering of Ag-Bi12GeO20-Bi2WO6 composite photocatalyst: Interface regulation and enhanced photocatalytic performance. Ceramics International, 2019, 45, 5249-5258.	4.8	14
86	Fully Air-Bladed High-Efficiency Perovskite Photovoltaics. Joule, 2019, 3, 402-416.	24.0	119
87	High-Mobility Hydrophobic Conjugated Polymer as Effective Interlayer for Air-Stable Efficient Perovskite Solar Cells (Solar RRL 1â^•2019). Solar Rrl, 2019, 3, 1970015.	5.8	1
88	Strain-engineering the anisotropic electrical properties of low-symmetry bilayer GeSe. Journal of Applied Physics, 2019, 125, .	2.5	5
89	Highâ€Mobility Hydrophobic Conjugated Polymer as Effective Interlayer for Airâ€Stable Efficient Perovskite Solar Cells. Solar Rrl, 2019, 3, 1800232.	5.8	36
90	Phaseâ€Controlled Synthesis of 1Tâ€MoSe <sub>2</sub> /NiSe Heterostructure Nanowire Arrays via Electronic Injection for Synergistically Enhanced Hydrogen Evolution. Small Methods, 2019, 3, 1800317.	8.6	67

#	Article	IF	CITATIONS
91	When MoS2 meets FeOOH: A "one-stone-two-birds'' heterostructure as a bifunctional electrocatalyst for efficient alkaline water splitting. Applied Catalysis B: Environmental, 2019, 244, 1004-1012.	20.2	144
92	Inâ€Plane Optical Anisotropy of Low‣ymmetry 2D GeSe. Advanced Optical Materials, 2019, 7, 1801311.	7.3	68
93	Air-Stable In-Plane Anisotropic GeSe <sub>2</sub> for Highly Polarization-Sensitive Photodetection in Short Wave Region. Journal of the American Chemical Society, 2018, 140, 4150-4156.	13.7	180
94	Particle-in-box nanostructured materials created via spatially confined pyrolysis as high performance bifunctional catalysts for electrochemical overall water splitting. Nano Energy, 2018, 48, 489-499.	16.0	90
95	Highly Boosted Microbial Extracellular Electron Transfer by Semiconductor Nanowire Array with Suitable Energy Level. Advanced Functional Materials, 2018, 28, 1707408.	14.9	17
96	Electrochemical Responsive Superhydrophilic Surfaces of Polythiophene Derivatives towards Cell Capture and Release. ChemPhysChem, 2018, 19, 2046-2051.	2.1	13
97	Highly π-extended copolymer as additive-free hole-transport material for perovskite solar cells. Nano Research, 2018, 11, 185-194.	10.4	24
98	In situ transformation of Cu2O@MnO2 to Cu@Mn(OH)2 nanosheet-on-nanowire arrays for efficient hydrogen evolution. Nano Research, 2018, 11, 1798-1809.	10.4	37
99	Self-terminated activation for high-yield production of N,P-codoped nanoporous carbon as an efficient metal-free electrocatalyst for Zn-air battery. Carbon, 2018, 128, 97-105.	10.3	69
100	From biological enzyme to single atomic Fe–N–C electrocatalyst for efficient oxygen reduction. Chemical Communications, 2018, 54, 1307-1310.	4.1	50
101	Congeneric Incorporation of CsPbBr <sub>3</sub> Nanocrystals in a Hybrid Perovskite Heterojunction for Photovoltaic Efficiency Enhancement. ACS Energy Letters, 2018, 3, 30-38.	17.4	106
102	Kinetically Controlled Coprecipitation for General Fast Synthesis of Sandwiched Metal Hydroxide Nanosheets/Graphene Composites toward Efficient Water Splitting. Advanced Functional Materials, 2018, 28, 1704594.	14.9	91
103	3D nanoporous Ni/V <sub>2</sub> O <sub>3</sub> hybrid nanoplate assemblies for highly efficient electrochemical hydrogen evolution. Journal of Materials Chemistry A, 2018, 6, 21452-21457.	10.3	38
104	Strain-engineering the electronic properties and anisotropy of GeSe <sub>2</sub> monolayers. RSC Advances, 2018, 8, 33445-33450.	3.6	9
105	Bimetal Prussian Blue as a Continuously Variable Platform for Investigating the Composition–Activity Relationship of Phosphides-Based Electrocatalysts for Water Oxidation. ACS Applied Materials & Interfaces, 2018, 10, 35904-35910.	8.0	28
106	Tuning the Optical Absorption Property of GeSe Thin Films by Annealing Treatment. Physica Status Solidi - Rapid Research Letters, 2018, 12, 1800370.	2.4	12
107	Carrier Dynamics Engineering for High-Performance Electron-Transport-Layer-free Perovskite Photovoltaics. CheM, 2018, 4, 2405-2417.	11.7	57
108	Scalable Solid‣tate Synthesis of Highly Dispersed Uncapped Metal (Rh, Ru, Ir) Nanoparticles for Efficient Hydrogen Evolution. Advanced Energy Materials, 2018, 8, 1801698.	19.5	149

#	Article	IF	CITATIONS
109	Self-supported metal sulphide nanocrystals-assembled nanosheets on carbon paper as efficient counter electrodes for quantum-dot-sensitized solar cells. Science China Chemistry, 2018, 61, 1338-1344.	8.2	7
110	Selfâ€Limited onâ€Site Conversion of MoO <sub>3</sub> Nanodots into Vertically Aligned Ultrasmall Monolayer MoS <sub>2</sub> for Efficient Hydrogen Evolution. Advanced Energy Materials, 2018, 8, 1800734.	19.5	112
111	A Twoâ€Dimensional Holeâ€Transporting Material for Highâ€Performance Perovskite Solar Cells with 20 % Average Efficiency. Angewandte Chemie, 2018, 130, 11125-11131.	2.0	25
112	A Twoâ€Dimensional Holeâ€Transporting Material for Highâ€Performance Perovskite Solar Cells with 20 % Average Efficiency. Angewandte Chemie - International Edition, 2018, 57, 10959-10965.	13.8	127
113	Scalable solid-state synthesis of coralline-like nanostructured Co@CoNC electrocatalyst for Zn–air batteries. Chemical Communications, 2018, 54, 8190-8193.	4.1	23
114	Hydrogen Evolution: Self-Limited on-Site Conversion of MoO3 Nanodots into Vertically Aligned Ultrasmall Monolayer MoS2 for Efficient Hydrogen Evolution (Adv. Energy Mater. 21/2018). Advanced Energy Materials, 2018, 8, 1870098.	19.5	1
115	Manipulation of facet orientation in hybrid perovskite polycrystalline films by cation cascade. Nature Communications, 2018, 9, 2793.	12.8	189
116	Thermodynamically Stable Orthorhombic γ-CsPbI <sub>3</sub> Thin Films for High-Performance Photovoltaics. Journal of the American Chemical Society, 2018, 140, 11716-11725.	13.7	308
117	Polar Solvent Induced Lattice Distortion of Cubic CsPbI <sub>3</sub> Nanocubes and Hierarchical Self-Assembly into Orthorhombic Single-Crystalline Nanowires. Journal of the American Chemical Society, 2018, 140, 11705-11715.	13.7	223
118	Size and Electronic Modulation of Iridium Nanoparticles on Nitrogen-Functionalized Carbon toward Advanced Electrocatalysts for Alkaline Water Splitting. ACS Applied Materials & Interfaces, 2018, 10, 22340-22347.	8.0	43
119	Alloying Strategy in Cu–In–Ga–Se Quantum Dots for High Efficiency Quantum Dot Sensitized Solar Cells. ACS Applied Materials & Interfaces, 2017, 9, 5328-5336.	8.0	87
120	Lamellar Metal Organic Framework-Derived Fe–N–C Non-Noble Electrocatalysts with Bimodal Porosity for Efficient Oxygen Reduction. ACS Applied Materials & Interfaces, 2017, 9, 5272-5278.	8.0	95
121	Tuning the branches and composition of PtCu nanodendrites through underpotential deposition of Cu towards advanced electrocatalytic activity. Journal of Materials Chemistry A, 2017, 5, 9014-9021.	10.3	55
122	Facile and Scalable Synthesis of Robust Ni(OH) <sub>2</sub> Nanoplate Arrays on NiAl Foil as Hierarchical Active Scaffold for Highly Efficient Overall Water Splitting. Advanced Science, 2017, 4, 1700084.	11.2	85
123	Crystallinityâ€Modulated Electrocatalytic Activity of a Nickel(II) Borate Thin Layer on Ni <sub>3</sub> B for Efficient Water Oxidation. Angewandte Chemie, 2017, 129, 6672-6677.	2.0	34
124	Crystallinityâ€Modulated Electrocatalytic Activity of a Nickel(II) Borate Thin Layer on Ni <sub>3</sub> B for Efficient Water Oxidation. Angewandte Chemie - International Edition, 2017, 56, 6572-6577.	13.8	271
125	Bilayer PbS Quantum Dots for Highâ€Performance Photodetectors. Advanced Materials, 2017, 29, 1702055.	21.0	189
126	Investigation of Physical and Electronic Properties of GeSe for Photovoltaic Applications. Advanced Electronic Materials, 2017, 3, 1700141.	5.1	81

#	Article	IF	CITATIONS
127	Electronic and Morphological Dual Modulation of Cobalt Carbonate Hydroxides by Mn Doping toward Highly Efficient and Stable Bifunctional Electrocatalysts for Overall Water Splitting. Journal of the American Chemical Society, 2017, 139, 8320-8328.	13.7	745
128	Facile Synthesis of <scp>Mo<sub>2</sub>C</scp> Nanocrystals Embedded in Nanoporous Carbon Network for Efficient Hydrogen Evolution. Chinese Journal of Chemistry, 2017, 35, 911-917.	4.9	12
129	Low-temperature aqueous solution processed ZnO as an electron transporting layer for efficient perovskite solar cells. Materials Chemistry Frontiers, 2017, 1, 802-806.	5.9	25
130	Three-dimensional nanostructured electrodes for efficient quantum-dot-sensitized solar cells. Nano Energy, 2017, 32, 130-156.	16.0	73
131	GeSe Thin-Film Solar Cells Fabricated by Self-Regulated Rapid Thermal Sublimation. Journal of the American Chemical Society, 2017, 139, 958-965.	13.7	238
132	Encased Copper Boosts the Electrocatalytic Activity of N-Doped Carbon Nanotubes for Hydrogen Evolution. ACS Applied Materials & amp; Interfaces, 2017, 9, 36857-36864.	8.0	75
133	Additive engineering for high-performance room-temperature-processed perovskite absorbers with micron-size grains and microsecond-range carrier lifetimes. Energy and Environmental Science, 2017, 10, 2365-2371.	30.8	157
134	Microbial-Phosphorus-Enabled Synthesis of Phosphide Nanocomposites for Efficient Electrocatalysts. Journal of the American Chemical Society, 2017, 139, 11248-11253.	13.7	70
135	Well-Defined Metal–O <sub>6</sub> in Metal–Catecholates as a Novel Active Site for Oxygen Electroreduction. ACS Applied Materials & Interfaces, 2017, 9, 28473-28477.	8.0	63
136	Selfâ€Templated Fabrication of MoNi <sub>4</sub> /MoO <sub>3â€</sub> <i><sub>x</sub></i> Nanorod Arrays with Dual Active Components for Highly Efficient Hydrogen Evolution. Advanced Materials, 2017, 29, 1703311.	21.0	437
137	Enhancing Electron and Hole Extractions for Efficient PbS Quantum Dot Solar Cells. Solar Rrl, 2017, 1, 1700176.	5.8	12
138	Co@N-CNTs derived from triple-role CoAl-layered double hydroxide as an efficient catalyst for oxygen reduction reaction. Carbon, 2016, 107, 162-170.	10.3	60
139	MoS <sub>2</sub> /CdS Nanosheets-on-Nanorod Heterostructure for Highly Efficient Photocatalytic H <sub>2</sub> Generation under Visible Light Irradiation. ACS Applied Materials & Interfaces, 2016, 8, 15258-15266.	8.0	426
140	Sodium chloride-assisted green synthesis of a 3D Fe–N–C hybrid as a highly active electrocatalyst for the oxygen reduction reaction. Journal of Materials Chemistry A, 2016, 4, 7781-7787.	10.3	88
141	Influence of <i>N</i> , <i>N</i> -Dimethylformamide Annealing on the Local Electrical Properties of Organometal Halide Perovskite Solar Cells: an Atomic Force Microscopy Investigation. ACS Applied Materials & Interfaces, 2016, 8, 26002-26007.	8.0	39
142	Cobalt carbide nanoprisms for direct production of lower olefins from syngas. Nature, 2016, 538, 84-87.	27.8	647
143	Promoting crystalline grain growth and healing pinholes by water vapor modulated post-annealing for enhancing the efficiency of planar perovskite solar cells. Journal of Materials Chemistry A, 2016, 4, 13458-13467.	10.3	58
144	Post-annealing of MAPbI <sub>3</sub> perovskite films with methylamine for efficient perovskite solar cells. Materials Horizons, 2016, 3, 548-555.	12.2	141

#	Article	IF	CITATIONS
145	Rational design and electron transfer kinetics of MoS2/CdS nanodots-on-nanorods for efficient visible-light-driven hydrogen generation. Nano Energy, 2016, 28, 319-329.	16.0	140
146	General Space-Confined On-Substrate Fabrication of Thickness-Adjustable Hybrid Perovskite Single-Crystalline Thin Films. Journal of the American Chemical Society, 2016, 138, 16196-16199.	13.7	205
147	Tuning the Fermi-level of TiO <sub>2</sub> mesoporous layer by lanthanum doping towards efficient perovskite solar cells. Nanoscale, 2016, 8, 16881-16885.	5.6	103
148	Pomegranate-like N,P-Doped Mo <sub>2</sub> C@C Nanospheres as Highly Active Electrocatalysts for Alkaline Hydrogen Evolution. ACS Nano, 2016, 10, 8851-8860.	14.6	575
149	Nitrogen, phosphorus and sulfur co-doped ultrathin carbon nanosheets as a metal-free catalyst for selective oxidation of aromatic alkanes and the oxygen reduction reaction. Journal of Materials Chemistry A, 2016, 4, 18470-18477.	10.3	93
150	Controlling the Cavity Structures of Twoâ€₽hotonâ€Pumped Perovskite Microlasers. Advanced Materials, 2016, 28, 4040-4046.	21.0	207
151	Understanding the High Activity of Fe–N–C Electrocatalysts in Oxygen Reduction: Fe/Fe <sub>3</sub> C Nanoparticles Boost the Activity of Fe–N <sub><i>x</i></sub> . Journal of the American Chemical Society, 2016, 138, 3570-3578.	13.7	1,549
152	Zn–Cu–In–Se Quantum Dot Solar Cells with a Certified Power Conversion Efficiency of 11.6%. Journal of the American Chemical Society, 2016, 138, 4201-4209.	13.7	537
153	Solvent-Assisted Preparation of High-Performance Mesoporous CH3NH3PbI3 Perovskite Solar Cells. Journal of Nanoscience and Nanotechnology, 2016, 16, 844-850.	0.9	1
154	Hierarchical Nanowire Arrays as Three-Dimensional Fractal Nanobiointerfaces for High Efficient Capture of Cancer Cells. Nano Letters, 2016, 16, 766-772.	9.1	122
155	Optoeletronic investigation of Cu2ZnSn(S,Se)4 thin-films & Cu2ZnSn(S,Se)4/CdS interface with scanning probe microscopy. Science China Chemistry, 2016, 59, 231-236.	8.2	5
156	Confining Iron Carbide Nanocrystals inside CN <sub><i>x</i></sub> @CNT toward an Efficient Electrocatalyst for Oxygen Reduction Reaction. ACS Applied Materials & Interfaces, 2015, 7, 11508-11515.	8.0	94
157	Microscopic Investigation of Grain Boundaries in Organolead Halide Perovskite Solar Cells. ACS Applied Materials & Interfaces, 2015, 7, 28518-28523.	8.0	173
158	Solvent-Induced Oriented Attachment Growth of Air-Stable Phase-Pure Pyrite FeS <sub>2</sub> Nanocrystals. Journal of the American Chemical Society, 2015, 137, 2211-2214.	13.7	56
159	Urchin-like Au@CdS/WO <sub>3</sub> micro/nano heterostructure as a visible-light driven photocatalyst for efficient hydrogen generation. Chemical Communications, 2015, 51, 13842-13845.	4.1	82
160	Insight into the Effect of Oxygen Vacancy Concentration on the Catalytic Performance of MnO <sub>2</sub> . ACS Catalysis, 2015, 5, 4825-4832.	11.2	244
161	Boosting the Open Circuit Voltage and Fill Factor of QDSSCs Using Hierarchically Assembled ITO@Cu <sub>2</sub> S Nanowire Array Counter Electrodes. Nano Letters, 2015, 15, 3088-3095.	9.1	86
162	Embedding Pt Nanocrystals in N-Doped Porous Carbon/Carbon Nanotubes toward Highly Stable Electrocatalysts for the Oxygen Reduction Reaction. ACS Catalysis, 2015, 5, 2903-2909.	11.2	221

Jin-Song Hu

#	Article	IF	CITATIONS
163	Physical vapor deposition of amorphous MoS <sub>2</sub> nanosheet arrays on carbon cloth for highly reproducible large-area electrocatalysts for the hydrogen evolution reaction. Journal of Materials Chemistry A, 2015, 3, 19277-19281.	10.3	97
164	Carbon-free Cu2ZnSn(S,Se)4 film prepared via a non-hydrazine route. Science China Chemistry, 2014, 57, 1552-1558.	8.2	3
165	ITO@Cu <sub>2</sub> S Tunnel Junction Nanowire Arrays as Efficient Counter Electrode for Quantum-Dot-Sensitized Solar Cells. Nano Letters, 2014, 14, 365-372.	9.1	118
166	In situ nitrogen-doped nanoporous carbon nanocables as an efficient metal-free catalyst for oxygen reduction reaction. Journal of Materials Chemistry A, 2014, 2, 10154.	10.3	73
167	Engineering self-assembled N-doped graphene–carbon nanotube composites towards efficient oxygen reduction electrocatalysts. Physical Chemistry Chemical Physics, 2014, 16, 13605-13609.	2.8	28
168	Enhanced stability and activity with Pd–O junction formation and electronic structure modification of palladium nanoparticles supported on exfoliated montmorillonite for the oxygen reduction reaction. Chemical Communications, 2014, 50, 6660.	4.1	27
169	Co/CoO/CoFe <sub>2</sub> O <sub>4</sub> /G nanocomposites derived from layered double hydroxides towards mass production of efficient Pt-free electrocatalysts for oxygen reduction reaction. Nanoscale, 2014, 6, 203-206.	5.6	80
170	Engineering the Interfaces of ITO@Cu <sub>2</sub> S Nanowire Arrays toward Efficient and Stable Counter Electrodes for Quantum-Dot-Sensitized Solar Cells. ACS Applied Materials & Interfaces, 2014, 6, 15448-15455.	8.0	24
171	Nanoparticle Facilitated Extracellular Electron Transfer in Microbial Fuel Cells. Nano Letters, 2014, 14, 6737-6742.	9.1	157
172	Probing single- to multi-cell level charge transport in Geobacter sulfurreducens DL-1. Nature Communications, 2013, 4, 2751.	12.8	73
173	Pd-induced Pt(iv) reduction to form Pd@Pt/CNT core@shell catalyst for a more complete oxygen reduction. Journal of Materials Chemistry A, 2013, 1, 14443.	10.3	33
174	Spaceâ€Confinementâ€Induced Synthesis of Pyridinic―and Pyrrolicâ€Nitrogenâ€Doped Graphene for the Catalysis of Oxygen Reduction. Angewandte Chemie - International Edition, 2013, 52, 11755-11759.	13.8	620
175	Integrated Prototype Nanodevices via SnO2 Nanoparticles Decorated SnSe Nanosheets. Scientific Reports, 2013, 3, 2613.	3.3	42
176	Self-deposition of Pt nanocrystals on Mn3O4 coated carbon nanotubes for enhanced oxygen reduction electrocatalysis. Journal of Materials Chemistry A, 2013, 1, 7463.	10.3	47
177	Facile Solution Synthesis and Photoelectric Properties of Monolithic Tin(II) Sulfide Nanobelt Arrays. Chemistry - an Asian Journal, 2013, 8, 2483-2488.	3.3	7
178	Hanging Pt hollow nanocrystal assemblies on graphene resulting in an enhanced electrocatalyst. Chemical Communications, 2012, 48, 10331.	4.1	43
179	Morphology control and shape evolution in 3D hierarchical superstructures. Science China Chemistry, 2012, 55, 2249-2256.	8.2	49
180	Wurtzite Cu2ZnSnSe4 nanocrystals for high-performance organic–inorganic hybrid photodetectors. NPG Asia Materials, 2012, 4, e2-e2.	7.9	116

#	ARTICLE	IF	CITATIONS
181	Anisotropic Photoresponse Properties of Single Micrometerâ€Sized GeSe Nanosheet. Advanced Materials, 2012, 24, 4528-4533.	21.0	229
182	Eco-friendly visible-wavelength photodetectors based on bandgap engineerable nanomaterials. Journal of Materials Chemistry, 2011, 21, 17582.	6.7	42
183	Bandgap Engineering of Monodispersed Cu <sub>2–<i>x</i></sub> S <sub><i>y</i></sub> Se <sub>1–<i>y</i></sub> Nanocrystals through Chalcogen Ratio and Crystal Structure. Journal of the American Chemical Society, 2011, 133, 18558-18561.	13.7	96
184	Probing electron transfer mechanisms in <i>Shewanella oneidensis</i> MR-1 using a nanoelectrode platform and single-cell imaging. Proceedings of the National Academy of Sciences of the United States of America, 2010, 107, 16806-16810.	7.1	138
185	Metal Octaethylporphyrin Nanowire Array and Network toward Electric/Photoelectric Devices. Journal of Physical Chemistry C, 2009, 113, 16259-16265.	3.1	25
186	Programmed Fabrication of Bimetallic Nanobarcodes for Miniature Multiplexing Bioanalysis. Analytical Chemistry, 2009, 81, 2815-2818.	6.5	12
187	Carbon Coated Fe <sub>3</sub> O <sub>4</sub> Nanospindles as a Superior Anode Material for Lithiumâ€lon Batteries. Advanced Functional Materials, 2008, 18, 3941-3946.	14.9	1,177
188	Tinâ€Nanoparticles Encapsulated in Elastic Hollow Carbon Spheres for Highâ€Performance Anode Material in Lithiumâ€Ion Batteries. Advanced Materials, 2008, 20, 1160-1165.	21.0	1,002
189	Ionâ€Transferâ€Based Growth: A Mechanism for CuTCNQ Nanowire Formation. Advanced Materials, 2008, 20, 4879-4882.	21.0	36
190	Synthesis of Hierarchically Structured Metal Oxides and their Application in Heavy Metal Ion Removal. Advanced Materials, 2008, 20, 2977-2982.	21.0	568
191	Nanostructured Materials for Electrochemical Energy Conversion and Storage Devices. Advanced Materials, 2008, 20, 2878-2887.	21.0	2,054
192	Electrodeposition of monodispersed metal nanoparticles in a nafion film: Towards highly active nanocatalysts. Electrochemistry Communications, 2008, 10, 814-817.	4.7	22
193	Facile synthesis of nanoporous anatase spheres and their environmental applications. Chemical Communications, 2008, , 1184.	4.1	146
194	Introducing Dual Functional CNT Networks into CuO Nanomicrospheres toward Superior Electrode Materials for Lithium-Ion Batteries. Chemistry of Materials, 2008, 20, 3617-3622.	6.7	270
195	Single and Tandem Axial <i>p-i-n</i> Nanowire Photovoltaic Devices. Nano Letters, 2008, 8, 3456-3460.	9.1	401
196	ZnOEP based phototransistor: signal amplification and light-controlled switch. Chemical Communications, 2008, , 2653.	4.1	40
197	Controllable crystalline structure of fullerenenanorods and transport properties of an individual nanorod. Journal of Materials Chemistry, 2008, 18, 328-332.	6.7	82
198	A simple method to synthesize layered double hydroxide nanoscrolls. Materials Research Bulletin, 2007, 42, 571-575.	5.2	26

#	Article	IF	CITATIONS
199	3D Flowerlike Ceria Micro/Nanocomposite Structure and Its Application for Water Treatment and CO Removal. Chemistry of Materials, 2007, 19, 1648-1655.	6.7	433
200	Facile solution synthesis of hexagonal Alq3 nanorods and their field emission properties. Chemical Communications, 2007, , 3083.	4.1	49
201	In-Situ Loading of Noble Metal Nanoparticles on Hydroxyl-Group-Rich Titania Precursor and Their Catalytic Applications. Chemistry of Materials, 2007, 19, 4557-4562.	6.7	156
202	Effect of Polycyclic Aromatic Hydrocarbons on Detection Sensitivity of Ultratrace Nitroaromatic Compounds. Analytical Chemistry, 2007, 79, 2179-2183.	6.5	26
203	Controllable Preparation of Submicrometer Single-Crystal C60Rods and Tubes Trough Concentration Depletion at the Surfaces of Seeds. Journal of Physical Chemistry C, 2007, 111, 10498-10502.	3.1	98
204	In Situ One-Step Method for Preparing Carbon Nanotubes and Pt Composite Catalysts and Their Performance for Methanol Oxidation. Journal of Physical Chemistry C, 2007, 111, 11174-11179.	3.1	127
205	Detection of VOCs and their concentrations by a single SnO2 sensor using kinetic information. Sensors and Actuators B: Chemical, 2007, 123, 454-460.	7.8	19
206	Functionalized carbon nanotubes as sensitive materials for electrochemical detection of ultra-trace 2,4,6-trinitrotoluene. Physical Chemistry Chemical Physics, 2006, 8, 3567.	2.8	66
207	Hierarchically Structured Cobalt Oxide (Co3O4):Â The Morphology Control and Its Potential in Sensors. Journal of Physical Chemistry B, 2006, 110, 15858-15863.	2.6	339
208	Electrochemical Sensor for Detecting Ultratrace Nitroaromatic Compounds Using Mesoporous SiO2-Modified Electrode. Analytical Chemistry, 2006, 78, 1967-1971.	6.5	204
209	Facile Synthesis of Pt Multipods Nanocrystals. Journal of Nanoscience and Nanotechnology, 2006, 6, 2031-2036.	0.9	4
210	Bis(ethylenedithio)tetrathiafulvalene Charge-Transfer Salt Nanotube Arrays. Advanced Materials, 2006, 18, 2753-2757.	21.0	17
211	Self-Assembled 3D Flowerlike Iron Oxide Nanostructures and Their Application in Water Treatment. Advanced Materials, 2006, 18, 2426-2431.	21.0	1,526
212	Mass Production and High Photocatalytic Activity of ZnS Nanoporous Nanoparticles. Angewandte Chemie - International Edition, 2005, 44, 1269-1273.	13.8	558
213	Self-Assembled Vanadium Pentoxide (V2O5) Hollow Microspheres from Nanorods and Their Application in Lithium-Ion Batteries. Angewandte Chemie - International Edition, 2005, 44, 4391-4395.	13.8	840
214	TiO2-Based Composite Nanotube Arrays Prepared via Layer-by-Layer Assembly. Advanced Functional Materials, 2005, 15, 196-202.	14.9	103
215	Tin/Platinum Bimetallic Nanotube Array and its Electrocatalytic Activity for Methanol Oxidation. Advanced Materials, 2005, 17, 746-750.	21.0	93
216	Self-Assembled Vanadium Pentoxide (V2O5) Hollow Microspheres from Nanorods and Their Application in Lithium-Ion Batteries ChemInform, 2005, 36, no.	0.0	0

#	Article	IF	CITATIONS
217	Nanoarchitectured metal film electrodes with high electroactive surface areas. Thin Solid Films, 2005, 484, 341-345.	1.8	23
218	A Simple Route to Platinum and Pt-Based Composite Nanotubes. Journal of Nanoscience and Nanotechnology, 2005, 5, 1929-1932.	0.9	3
219	Niâ^'Pt Multilayered Nanowire Arrays with Enhanced Coercivity and High Remanence Ratio. Inorganic Chemistry, 2005, 44, 3013-3015.	4.0	81
220	Three-Dimensional Self-Organization of Supramolecular Self-Assembled Porphyrin Hollow Hexagonal Nanoprisms. Journal of the American Chemical Society, 2005, 127, 17090-17095.	13.7	302
221	Controllable Pt Nanoparticle Deposition on Carbon Nanotubes as an Anode Catalyst for Direct Methanol Fuel Cells. Journal of Physical Chemistry B, 2005, 109, 22212-22216.	2.6	454
222	Pt Hollow Nanospheres: Facile Synthesis and Enhanced Electrocatalysts. Angewandte Chemie - International Edition, 2004, 43, 1540-1543.	13.8	662
223	Pt Hollow Nanospheres: Facile Synthesis and Enhanced Electrocatalysts ChemInform, 2004, 35, no.	0.0	0
224	Interface Assembly Synthesis of Inorganic Composite Hollow Spheres. Journal of Physical Chemistry B, 2004, 108, 9734-9738.	2.6	62
225	Controllable AuPt bimetallic hollow nanostructures. Chemical Communications, 2004, , 1496.	4.1	121
226	Electronic Characteristics of Au-Mercaptohexadecanoic Acid-Au Junction in a Capillary. Journal of Nanoscience and Nanotechnology, 2004, 4, 1081-1084.	0.9	0
227	Highly Dispersed Metal Nanoparticles in Porous Anodic Alumina Films Prepared by a Breathing Process of Polyacrylamide Hydrogel. Chemistry of Materials, 2003, 15, 4332-4336.	6.7	61